PNNL-11600
UC-2030

Thermal and Radiolytic Gas Generation from Tank 241-S-102 Waste

C. M. King
L. R. Pederson
S. A. Bryan

July 1997

Prepared for
the U.S. Department of Energy
under Contract DE-ACO6-76RLO 1830

Pacific Northwest National Laboratory
Richland, Washington 99352

DISCLAIMER

PACIFIC NORTHWEST NATIONAL LABORATORY
operated by
BATTELLE
for the
UNITED STATES DEPARTMENT OF ENERGY
under Contract DE-AC06-76RLO 1830

Printed in the United States of America

Available to DOE and DOE contractors from the Office of Scientific and Technical Information, P.O. Box 62, Oak Ridge, TN 37831; prices available from (615) 576-8401.

Available to the public from the National Technical Information Service, U.S. Department of Commerce, 5285 Port Royal Rd., Springfield, VA 22161


This document was printed on recycled paper.

Executive Summary

This report summarizes progress in evaluating thermal and radiolytic rate parameters for flammable gas generation in Hanford single-shell tank wastes based on the results of laboratory tests using actual waste from Tank 241-S-102 (S-102). Work described in this report was conducted at Pacific Northwest National Laboratory (PNNL)[(a)] for the Flammable Gas Safety Project, whose purpose is to develop information to support Fluor Daniel Hanford (FDH) and its Project Management Hanford Contract (PHMC) subcontractors in their efforts to ensure the safe interim storage of wastes at the Hanford Site. This work is related to gas generation studies being performed at Georgia Institute of Technology (GIT) under subcontract to PNNL, using simulated wastes, and to studies being performed at Numatec Hanford Corporation (formerly Westinghouse Hanford Company) using actual wastes.

The results of gas generation from Tank S-102 waste under thermal and radiolytic conditions are described in this report. The accurate measurement of gas generation rates in actual waste from highly radioactive waste tanks is needed to assess the potential for producing and storing flammable gases within the waste tanks. This report addresses the gas generation capacity of the waste from Tank S-102, a waste tank listed as high priority by the Flammable Gas Safety Program due to its potential for flammable gas accumulation above the flammability limit (Johnson et al. 1997).

The main objective of this work is to establish the identity and stoichiometry of degradation products formed in actual tank wastes by thermal and radiolytic processes as a function of temperature. The focus of the gas generation tests on Tank S-102 samples is on the effect of temperature on the composition and rate of gas generation. Generation rates of nitrogen, nitrous oxide, hydrogen, and methane increased with increased temperature, though at different rates. The composition of the product gas mixture varied with temperature. The fraction of hydrogen decreased with increased temperature in the range 60 to 120°C, the fraction of nitrous oxide decreased slightly, and the fraction of nitrogen and methane increased.

The consequences of changes in relative concentrations of gases are seen in differences in activation energies for the production of these gases. Arrhenius treatment of the rate data revealed activation parameters for the gas generation from Tank S-102 based on the rate of formation of each component gas in the systems.

A second component of this work is the study of the gas generation capacity of Tank S-102 waste in the presence of an external gamma source. The radiolytic G-values for gas generation are 0.017 ±0.004 molecules/100eV for hydrogen, 0.009 ±0.003 molecules/100eV for nitrous oxide, 0.009 ±0.003 molecules/100eV for nitrogen, and 0.0005 ±0.0002 molecules/100eV for methane.

(a) Pacific Northwest National Laboratory is operated by Battelle for the U.S. Department of Energy under Contract DE-AC06-76RLO 1830.

The waste is being analyzed for specific organic components. Separate organic analysis samples were taken before and after heating and radiolysis to help identify the organic species responsible for gas generation. By following the specific organic species present and their concentration changes as a function of heating and irradiation, along with the results of measurements of the gases formed during the heating and irradiation treatments, a better understanding of the organics responsible for gas generation is possible. Long-term gas generation is being investigated using S-102 material under actual tank temperature and dose rate conditions. These results and those for organic and ammonia analyses will be reported in a subsequent document.

Using the thermal and radiolytic activation parameters for gas generation in actual tank waste, the rate of hydrogen generation in the entire tank can be estimated for Tank S-102. The rate of hydrogen generation in tank material is the sum of thermal and radiolytic rates. The thermal hydrogen generation rate at 41°C is 8.6E-8 mol/kg/day, and the radiolytic rate is 1.6E-7 mol/ kg/day, which results in a total hydrogen generation rate of 1.0 ± 0.2 mol/day for the best estimate of the tank conditions. This compares favorably with the estimate made using tank breathing rates and gas grab samples (3.8 ± 4 mol/day).[a] The values for hydrogen generation from Tank S-102 are smaller than previously measured generation rates from Tank 241-SY-103 (~10 mol/day).

Reference

Johnson GD, WB Barton, RC Hill, JW Brothers, SA Bryan, PA Gauglitz, LR Pederson, CW Stewart, and LH Stock. 1997. *Flammable Gas Project Topical Report.* HNF-SP-1193 Rev. 2, Project Hanford Management Contractor, Richland, Washington.

(a) Barton WB. 1997. *Field Estimated Gas Generation Rates.* Presented at Safety-Controls by Performance Evaluation (SCOPE) Meeting, April 28–May 2, 1997. Lockheed Martin Hanford Corporation, Richland, Washington.

Contents

Figures

Tables

1.0 Introduction

This report describes the research performed to measure gas generation from actual waste taken from a composite sample representing Tank S-102 (S-102). Results of thermal and radiolytic gas generation from Tank S-102 waste are discussed. Work described in this report is being conducted at Pacific Northwest National Laboratory (PNNL) for the Hanford Tank Waste Safety Flammable Gas Program, whose purpose is to develop information needed to support the interim safe storage of nuclear and chemical wastes at the Hanford Site. This work, requested by Fluor Daniel Hanford (FDH), started in FY 1996 and continues into FY 1997.

The gas generation tests on Tank S-102 samples are focused first on finding the effect of temperature on gas generation, and second on measuring gas generation from irradiation of Tank S-102 samples with an external radiation source (^{137}Cs capsule). This work was detailed in the Gas Generation Test Plan submitted to the Flammable Gas Program Office prior to the start of gas generation testing.[a] There were no deviations from the stated test plan.

The tank waste samples and radiation source are contained within a hot cell. Gas measurement equipment is contained in an adjacent hood, attached to the reaction vessels by small-diameter stainless steel tubing. The tests establish gas generation rates from actual waste samples as a function of temperature with and without irradiation. From these results, thermal activation energies can be calculated that will allow gas generation rates at other temperatures to be calculated. G-values for the radiolytic gas generation component are also derived from these data.

To assess the effects of temperature on the gas generation from S-102 Tank waste samples, experiments were performed in duplicate at four temperatures (60, 80, 100, and 120°C) for a total of eight reactions (four temperatures x two replicates). The effects of radiation on gas generation were assessed by the addition of an external ^{137}Cs gamma capsule to the Tank S-102 samples. For comparison, the irradiation experiments were performed in duplicate at the same temperatures as the "thermal-only" experiments (60, 80, 100, and 120°C). In the thermal tests we measured activation parameters (energies of activation [Laidler 1987]) for gas generation, and in the radiolytic experiments we determined the G-values (Spinks and Woods 1991) for gas generation. These parameters allow for the determination of gas generation rates of the principal gas components within Tank S-102 under current and future conditions.

Section 2 of this report describes the gas generation test samples and the experimental conditions and equipment used for the tests. Section 3 presents the results and a discussion of the gas generation experiments. The work is summarized in Section 4, and Section 5 contains the references cited.

(a) Bryan SA. 1996. *Test Plan: Tank S-102 Gas Generation Testing.* TWSFG97.11, Pacific Northwest National Laboratory, Richland, Washington.

2.0 Experimental Methods for Gas Measurements

Gas generation tests on actual radioactive tank waste were conducted at PNNL's High Level Radiochemistry Facility in the 325 Building (325A HLRF). The material examined was provided by the Characterization program, which obtained the core samples from Tank S-102. Gas generation measurements were made using reaction vessels and a gas manifold system similar to that used in earlier studies with simulated waste (Bryan and Pederson 1995) and described in an earlier report detailing work with actual waste (Bryan et al. 1996).

A description of the Tank S-102 test material is included in Section 2.1. A description of the experimental test conditions is given in Section 2.2. The self-dose rate from the radionuclide inventory of Tank S-102 samples was calculated to assess the amount of radiolytically induced gas from internal radiolytic sources. These calculations are included in Section 2.3.

2.1 Tank S-102 Test Material

The Tank Waste Remediation System Characterization program obtained core samples from Tank S-102. The tank contains 15 kL of sludge and 2,063 kL of saltcake; the sludge and saltcake contain 871 kL of drainable interstitial liquid (Hanlon 1997). Segments of these cores were separated into subsegments, which were homogenized (Eggers 1996). Some of these subsegments were sent to the 325A HLRF. The available subsegments were combined into a composite sample using the amounts shown in Table 1. The material was mixed with a spatula to obtain homogeneity (it was too thick to be mixed by a high-speed blender). The composite and subsegments resemble wet, dark gray, sticky sand. The main components in the waste averaged from the core data from S-102 are sodium, 190 mg/g; nitrate, 302 mg/g; phosphate, 44 mg/g; nitrite, 33 mg/g; aluminum, 14 mg/g; sulfate, 8.9 mg/g; and oxalate, 7.5 mg/g (Eggers 1996).

Table 1. Composition of Composite S-102 Waste Sample Used in Gas Generation Testing (uh = upper half segment, lh = lower half segment, 3/4 = third quarter segment)

Core	Segment	Distance (segment) from bottom of tank, m	Texture	Amount, g
125	4-uh	3.84	Saltcake	13.69
125	4-lh	3.60	Saltcake	45.90
125	5-lh	3.12	Saltcake	40.00
125	6-3/4	2.88	Saltcake	28.97
130	6B-lh	2.64	Damp saltcake	28.20
125	7-lh	2.16	Damp saltcake	48.45
130	9-uh	1.44	Sludge	25.29
125	9-lh	1.20	Sludge	51.07
130	10-uh	0.96	Sludge	24.95
125	10-lh	0.72	Sludge	59.80
130	11-lh	0.24	Mixture sludge/saltcake	68.13
Total				434.43

2.2 Experimental Conditions and Equipment

Gas generation measurements were made using reaction vessels and a gas manifold system similar to those used in previous studies on simulated and actual wastes (Bryan et al. 1994, 1995, 1996). The reaction vessels inside the hot cell are connected to a gas manifold outside the hot cell by small-diameter stainless steel tubing. Each vessel has a separate pressure transducer on the gas manifold line. The entire surface of the reaction system exposed to the waste sample is stainless steel, except for a gold-plated copper gasket sealing the flange at the top of the reaction vessel. A drawing of the reaction vessel showing the placement of the thermocouples within the reaction vessel, as well as placement of thermocouples at various locations on the reaction vessel, is shown as Figure 1. A schematic diagram of the gas manifold system is shown in Figure 2. Temperatures and pressures are recorded every 10 seconds on a Campbell Scientific CR10 data-logger. Every 20 minutes an average of the data is taken and saved in a computer file.

The reaction vessels were constructed of 304 stainless steel. The reaction space of the vessel is a cylinder approximately 5/8 in. in diameter by 8-1/4 in. high. Each vessel was wrapped in heating tape and insulated. Two thermocouples were attached to the external body of the reaction vessel to allow for temperature control and over-temperature protection. Two thermocouples were inserted through the lid of the vessel. The thermocouple centered in the lower half of the vessel monitors the temperature of the liquid phase. The thermocouple centered in the upper half monitors the gas phase temperature within the reaction vessel. The reaction vessels were placed in a hot cell and connected by a thin (0.0058 cm inside diameter) tube to the gas manifold outside the hot cell. A stainless steel filter (60-micrometer pore size, Nupro®) protected the tubing and manifold from contamination. A thermocouple also was attached to this filter.

Total moles of gases in the system were calculated from the pressure, temperature, and volume of each thermal region of the gas phase using the ideal gas law relationship: $moles_{total} = moles_{vessel} + moles_{filter} + moles_{manifold\ and\ tubing}$. The manifold and filter volumes were determined from pressure/volume relationships using a calibrated gas manifold system. The manifold volume (the pressure sensor, valves, and miscellaneous fittings) was 3.99 mL. The filter volume was 1.34 mL. The tubing volume was 1.715 mL (by calculation). The cap stem (the tube from vessel to filter) has a volume of 0.20 mL; half of that was added to the filter volume, giving 1.44 mL, and half was added to the vessel volumes. The volume of each vessel was determined gravimetrically by filling it with water. These volumes are recorded in Table 2, along with the mass of waste added to each vessel and the gas phase volume in the vessel after the sample was added. The density of the material was measured as 1.64 g/mL (Eggers 1996). The reproducibility of the molar gas determination using this manifold system has been determined experimentally, and a detailed discussion of this is included in Bryan et al. (1996). The relative standard deviation for quantitative gas phase measurements conducted over a time frame similar to that of the gas generation tests was typically less than 2%.

Gas solubilities of nitrogen, hydrogen, methane, and nitrous oxide have been measured on simulated waste systems similar in composition to S-102 waste (Pederson and Bryan 1996). For these gases, less than 0.01% of the total gas inventory will be dissolved or adsorbed in the

condensed phase, and loss of these gases due to solubility can be ignored. Solubility of ammonia is more appreciable in these systems, and solid-liquid phase ammonia measurements are being performed; these will be reported in a subsequent document.

An atmospheric pressure gauge was attached to the data-logger. The pressure in each system is given by the sum of the atmospheric pressure and the relative pressure in each system. Helium was used as a cover gas; this allows using the measured amount of argon in gas samples as an indicator of how much nitrogen from air has leaked into the system (the N_2:Ar ratio in air is 83.6:1). The nitrogen produced in the vessel is the total nitrogen minus atmospheric nitrogen. The helium used in this study was analyzed independently by mass spectrometry and determined to contain no impurities in concentrations significant enough to warrant correction.

At the start of a run, each system was purged by no less than 10 cycles of pressurizing with helium at 40 psi (276 kPa) and venting to the atmosphere. The systems were left at atmospheric pressure, about 745 mm Hg (99.3 kPa) prior to sealing. The sample portion of the manifold was then isolated (valves V1 and V2 closed, see Figure 2) for the remainder of the run. The vessels were then heated, adjusting the set points to keep the material within 1°C of the desired temperature. The set temperatures were 60, 80, 100 and 120°C. The temperature of the gas phase was 10 25°C lower than that of the solid-liquid sample phase.

At the end of each run, the vessels were allowed to cool overnight, and then a sample of the gas was taken. The metal gas collection bottles had a volume of approximately 75 mL and were equipped with a valve. The bottle, after being evacuated overnight at high vacuum, was attached to the gas sample port. Air was removed from the region between valves V2 and V5 (Figure 2) using a vacuum pump. This region was filled with gas from the reaction vessel and evacuated a second time to remove any residual air. After the collection bottle was removed, the bottle and sample port were surveyed for radioactive contamination. No contamination was found during these experiments.

We assume that gases in the reaction system are well mixed, a reasonable assumption. Samples are withdrawn through the capillary line into an evacuated bulb. The volume of the sampling bulb was approximately five times that of the gas reaction vessel. The reaction vessel was repurged with inert cover gas after each sampling event and before the next reaction sequence. For the irradiation experiments, the gamma source was removed from the experimental matrix during gas sampling events. In the irradiated and heated experiments, the time of irradiation was the same as sample heating.

Analysis of the composition of the gas phase of each reaction vessel after each run was performed according to analytical procedure PNNL-MA-599 ALO-284 Rev 1, by staff of the Mass Spectroscopy Facility operated by PNNL and located in the 325 Building. The amount of a specific gas formed during heating is given by the mole percent of each gas multiplied by the total moles of gas present in a system.

Duplicate samples, which were run in separate reaction vessels and sampled independently at each temperature, were used to assess the reproducibility and uncertainty of the rate parameters.

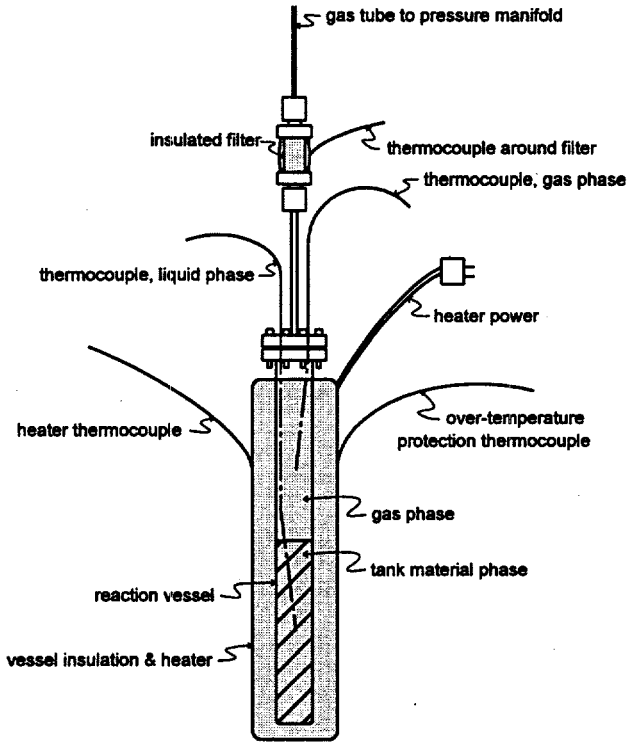

Figure 1. Reaction Vessel Used in Small-Scale Gas Generation Tests

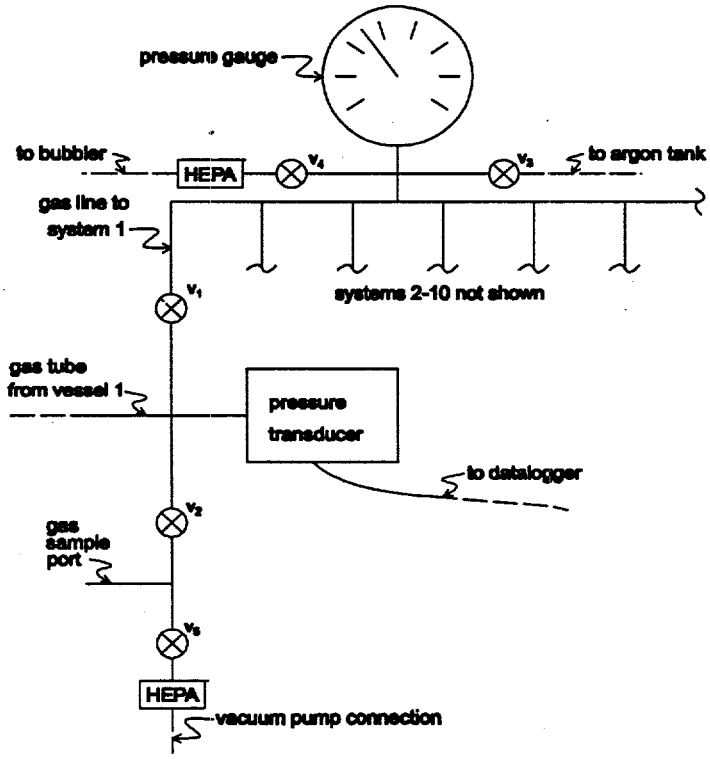

Figure 2. Diagram of Pressure Manifold System Used in Gas Generation Tests

Table 2. Sample Masses and Vessel Volumes Used In Small-Scale Gas Generation Tests Using Tank S-102 Wastes

	Thermal							
System	1	2	3	4	5	6	7	8
Temperature	60°C	60°C	80°C	80°C	100°C	100°C	120°C	120°C
Sample mass, g	20.58	18.67	19.31	19.65	18.69	19.37	19.567	18.97
Vessel volumes								
total, mL	29.80	29.75	29.80	28.91	29.70	29.80	29.22	29.70
gas phase, mL	17.25	18.37	18.02	16.93	18.31	17.99	17.29	18.13

	Radiolytic							
System	9	10	11	12	13	14	15	16
Temperature	60°C	60°C	80°C	80°C	100°C	100°C	120°C	120°C
Sample mass, g	18.10	18.89	19.93	19.09	19.00	18.81	18.47	19.41
Vessel volumes								
total, mL	29.30	29.35	29.22	29.80	29.67	29.19	29.18	29.25
gas phase, mL	18.65	18.24	17.49	18.57	18.49	18.12	18.31	17.83

2.3 Self-Dose Rate from Radionuclide Inventory in Tank S-102 Samples

Gamma dose rates were calculated by PNNL's Health Protection Department using the program MCNP version 4A (Monte Carlo N-Particle Transport Code System) (Briesmeister 1993). This program uses the Monte Carlo method, in which a radiation particle or photon is emitted in random directions from random locations in the sample. The probabilities of the radiation being absorbed by the sample and of its being reflected from the container wall back into the sample are known (Kocher 1981). Input to the program includes the composition of the vessel walls, the composition of the bulk of the sample, and the radionuclides present. The output is the amount of radiation absorbed by the sample averaged over the entire sample.

The gamma dose was calculated for the ^{137}Cs content in Tank S-102 material when in the tank and when in a reaction vessel. The tank material contains, besides water, 85,500 mg/g nitrogen, 15,600 μg/g phosphorus, 2,590 μg/g sulfur, 501,600 μg/g oxygen, 22,800 μg/g hydrogen (in hydroxide), 98.8 μCi/g ^{137}Cs, and 17.4 μCi/g ^{90}Sr based on sample analysis (Eggers 1996). Core segments 7 and 9 were the only separate segments analyzed for radionuclides. Two core composites, one containing saltcake (cores 1-7) and a second containing sludge (cores 9-11), were prepared and analyzed for radionuclides. The amounts of ^{137}Cs and ^{90}Sr were based on a weighted average of these two core composites (Eggers 1996). The tank was modeled as a cylinder with a diameter of 22.9 m, a height of 5.009 m, a 6.35-mm-thick steel wall, and 0.38 m of concrete around the outside. The reaction vessel was modeled as a cylinder with an inside radius of 0.794 cm, a height of 7.43 cm, and 0.127-cm-thick iron walls. The total dose rates averaged over the entire volumes were 207 R/h in the tank and 96 R/h in the vessel. The contributions from betas and electrons are given in Table 3. It was assumed that all beta and

Table 3. Beta and Secondary Electron Self Dose Rates from ^{137}Cs and ^{90}Sr Inventory in Tank S-102 Test Samples

Radionuclide	R/h
^{137}Cs	36.0
^{137m}Ba[(a)]	12.6
^{90}Sr	7.25
^{90}Y[(a)]	34.63
Total	90.5

(a) The ^{137m}Ba and ^{90}Y are daughters of ^{137}Cs and ^{90}Sr, respectively

electron energy was deposited in the sample when estimating the total dose rate (Table 4). For comparison, the total dose rate in Tank 241-SY-103 (SY-103) was calculated to be 444 R/h (Bryan et al. 1996). Fricke dosimetry was used to determine the dose rate in a reaction vessel with the ^{137}Cs capsule placed in the middle of the vessel holder, as described previously.[(a)] The dose rate received by a solution within the reaction vessel from the ^{137}Cs capsule was 37,400 R/h (average of five determinations) with a relative standard deviation of 6%.

Table 4. Calculated Self Dose Rates in Tank S-102 and in Test Vessel

	Gamma, R/h	Beta/Electron, R/h	Total, R/h
Tank	116.2	90.5	206.7
Vessel	5.2	90.5	95.7

(a) Bryan SA. 1996. *Test Plan: Tank S-102 Gas Generation Testing.* TWSFG97.11, Pacific Northwest National Laboratory, Richland, Washington.

3.0 Gas Generation from Tank S-102 Waste Samples

Waste stored in high-level waste tanks on the Hanford Site produces gas as a function of the thermal and radiolytic aging of its components. To assess the relative contributions of thermal versus radiolytic components of gas generation, we measured gas generation from Tank S-102 waste material under both thermal and radiolytic conditions. By isolating and measuring the thermal and radiolytic components of the gas generation, we can then predict the gas generation behavior of the waste under current tank conditions or under new conditions that may arise over time. This information has broad application and can be extended for use in other tanks or under other tank conditions.

The composition of the gases and generation rates for gas evolution under thermal and radiolytic conditions is described in Section 3.1. Thermal activation parameters from standard Arrhenius treatment of data and G-value determinations from the radiolytic experiments are reported in Section 3.2. A comparison of gas generation rates from S-102 and SY-103 wastes is presented in Section 3.3.

3.1 Composition and Rates of Gas Generation from Tank S-102 Waste

Gas generation from Tank S-102 waste was studied under both thermal and radiolytic conditions. Gases were produced thermally by heating material in the reaction vessels at 60, 80, 100, and 120°C. The radiolytic gas generation was measured by placing an external source of ^{137}Cs radiation (gamma capsule) adjacent to the reaction vessels while maintaining the temperature of each reaction vessel at the same level as the thermal-only experiments.

This section is divided into two subsections. The first details the results of gas generation from Tank S-102 waste under thermal conditions; the second details the radiolytic gas generation from S-102 waste.

3.1.1 Thermal Gas Generation from Tank S-102 Waste

This section contains the thermal gas generation data produced by heating material in the reaction vessels at 60, 80, 100, and 120°C. Thermal reactions were run in duplicate at each temperature. For each temperature, fresh Tank S-102 material was placed into a separate reaction vessel (see Table 2). For each reaction vessel, three to five samples of the generated gases were taken during the course of each reaction sequence. Gas generation rates were determined from the heating time, percent composition of the gas, and total moles of gas in each system when the sample was taken (Table 5) and from the mass of tank material present in each reaction vessel (Table 2). The time each vessel was heated between sampling events is given in Tables 5 and 6. In these tables, the individual runs are identified by a number and letter. The number identifies the reaction vessel, and the letter identifies the gas sampling event. For example, entries for runs 1a and 2a give data at the first gas sampling event for vessels 1 and 2, which happen to be duplicates at 60°C.

Table 5. Total Moles of Gas Present in Each Thermal System at Time of Sampling

Run	Time, hr	60°C	Run	Time, hr	80°C	Run	Time, hr	100°C	Run	Time, hr	120°C
1a	475	0.0462	3a	146	0.0521	5a	98	0.0562	7a	24	0.0512
1b	531	0.0451	3b	343	0.0526	5b	192	0.0530	7b	53	0.0496
1c	533	0.0460	3c	410	0.0503	5c	195	0.0521	7c	149	0.0522
						5d	410	0.0528	7d	155	0.0501
									7e	410	0.0534
2a	475	0.0533	4a	146	0.0496	6a	98	0.0538	8a	24	0.0321
2b	531	0.0517	4b	343	0.0481	6b	192	0.0500	8b	53	0.0549
2c	533	0.0525	4c	410	0.0488	6c	195	0.0488	8c	149	0.0555
						6d	410	0.0507	8d	155	0.0539
									8e	410	0.0555

The mole percent composition of the gas sampled at the end of each run is given in Table 6. Of more interest is the composition of gas that is generated; this composition is presented below the entry for each run, and is shaded gray. The composition of gas formed during heating is derived from the composition of sampled gas by excluding the helium cover gas, argon, nitrogen (from atmospheric contamination), and oxygen. For example, if analysis found 80% helium, 15% nitrous oxide, and 5% hydrogen, the composition of gas formed by excluding helium would be 75% N_2O and 25% H_2.

Since argon was not added as a cover gas (and was not produced from the waste) it was used as a tag indicator for atmospheric contamination. Any nitrogen present can come from nitrogen generated from the waste and/or from atmospheric contamination. The percent nitrogen generated is given by the percent nitrogen found minus 83.6 times the percent argon in the sample (the ratio of nitrogen to argon in dry air is 83.6). The rate of oxygen generation cannot be determined by the present experiment because tank material consumes oxygen when it is heated (Person 1996). The percent oxygen found in the samples was always less than expected from the amount of argon present, indicating that it was indeed being consumed.

The detection limit by mass spectrometry for argon is 10 ppm (0.001%). Near this level traces of organic gases are present and give a false positive signal for argon, which in turn leads to a slight overestimate of how much atmospheric gas (nitrogen) leaked into each reaction vessel. This overestimate was usually greater than the amount of nitrogen generated from the tank material. Due to this overestimate of argon (and hence nitrogen) and the low nitrogen generation rate from these waste samples, it appeared that nitrogen was consumed rather than produced in all runs except 7e and 8e. These two runs were at the highest reaction temperature, 120°C, and were heated longer than initially planned so that measurable amounts of nitrogen would be formed. The amount of nitrogen present at 100°C was estimated from runs 5d and 6d by assuming that all the measured argon (0.002 and 0.004%) was a false positive from organic interference. These two runs were chosen because they had the least atmospheric contamination

Table 6. Mole Percent Composition of Thermal Gas Sampled (including helium) and of Gas Formed (shaded), and Heating Times for Duplicate Systems at Four Temperatures (no external radiation source was used for these samples)

	Mole Percent of Gas Formed at 60°C										
Run	He	Ar	N_2	H_2	N_2O	CH_4	O_2	NH_3[a]	NO_x	$C_2H_{2,4,or\,6}$	Time, hr
1a	99.65	0.005	0.238	0.057	0.016		0.030				475
				78	22						
1b	99.78	0.004	0.147	0.053	0.007		0.008				531
				88	12						
1c	99.83	0.003	0.101	0.032	0.006		0.023				533
				84	16						
2a	99.52	0.004	0.304	0.097	0.023	0.003	0.048				475
				79	19	2					
2b	99.71	0.005	0.165	0.077	0.014	0.003	0.020				531
				82	15	3					
2c	99.83	0.002	0.063	0.072	0.011	0.003	0.018				533
				84	13	3					

	Mole Percent of Gas Formed at 80°C										
Run	He	Ar	N_2	H_2	N_2O	CH_4	O_2	NH_3[a]	NO_x	$C_2H_{2,4,or\,6}$	Time, hr
3a	95.3	0.109	3.63	0.060	0.030	0.004	0.82				146
				64	32	4					
3b	99.46	0.011	0.301	0.153	0.033	0.013	0.023		0.008		343
				74	16	6			4		
3c	99.45	0.004	0.186	0.239	0.033	0.022	0.024		0.04		410
				69	10	6			12		
4a	96.3	0.062	2.82	0.079	0.034	0.007	0.66				146
				66	28	6					
4b	99.40	0.010	0.299	0.192	0.038	0.021	0.036				343
				76	15	8					
4c	99.46	0.003	0.143	0.255	0.043	0.031	0.017	0.03	0.02		410
				66	11	8		8	5		

(a) Measurements for ammonia are for gas phase only and do not include ammonia dissolved in the solid-liquid phase, which will be reported in a subsequent document.

at 100°C based on measured amounts of nitrogen and argon. The correction for false positive for argon (0.002%) was applied to the data before applying the Ar/N_2 correction.

Ammonia concentrations in the samples, as measured by gas-phase mass spectroscopy, are included in Table 6. These are listed as gas phase measurements because a large fraction of ammonia is expected to remain in the solid-liquid phase (Pederson and Bryan 1996). Ammonia analyses of the solid-liquid phase are currently being performed and will be reported in another document. Consideration of wall adsorption effects on ammonia concentration measurements will be included with final ammonia results. The concentration of carbon monoxide in the

Table 6 (contd)

Mole Percent of Gas Formed at 100°C

Run	He	Ar	N_2	H_2	N_2O	CH_4	O_2	NH_3[a]	NO_x	$C_2H_{2,4,or\ 6}$	Time, hr
5a	93.3	0.177	5.1	0.144	0.091	0.023	1.09				98
				56	35	9					
5b	96.4	0.037	2.57	0.321	0.029	0.063	0.59				192
				78	7	15					
5c	99.2	0.007	0.219	0.41	0.031	0.093	0.030	0.002	0.005		195
				76	6	17		0.4	0.9		
5d	98.65	0.004	0.135	0.88	0.055	0.239	0.017		0.02		410
			10	64	4.0	17			1		
6a	79.2	0.192	16.2	0.225	0.090	0.046	4.03				98
				62	25	13					
6b	96.1	0.032	2.59	0.387	0.056	0.091	0.65		0.059		192
				65	9	15			10		
6c	99.3	0.003	0.187	0.284	0.053	0.072	0.033		0.064		195
				60	11	15			14		
6d	98.37	0.002	0.16	1.01	0.083	0.31	0.022		0.04		410
			10	61	5.1	14			2		

Mole Percent of Gas Formed at 120°C

Run	He	Ar	N_2	H_2	N_2O	CH_4	O_2	NH_3[a]	NO_x	$C_2H_{2,4,or\ 6}$	Time, hr
7a	96.6	0.043	2.24	0.448	0.131	0.24	0.287	0.02		0.01	24
				52.2	15	28		2		1	
7b	95.2	0.034	2.69	0.93	0.057	0.438	0.67		0.007	0.001	53
				65	4.0	31			0.5	0.1	
7c	94.0	0.031	2.38	1.67	0.124	1.17	0.56		0.050		149
				55	4.1	39			1.7		
7d	96.1	0.013	0.98	1.07	0.413	1.15	0.024	0.007	0.210	0.004	155
				37	14	40.3		0.2	7.4	0.1	
7e	90.7	0.011	1.39	2.42	2.45	2.53	0.143	0.02	0.34	0.005	410
			5.7	29.3	30	30.6		0.2	4.1	0.06	
8a	94.3	0.075	4.45	0.363	0.178	0.13	0.48	0.01		0.01	24
				51.8	25	19		1		1	
8b	94.7	0.041	3.38	0.78	0.068	0.327	0.69	0.003	0.014	0.001	53
				65	5.7	27		0.3	1.2	0.1	
8c	93.6	0.037	2.85	1.46	0.099	1.02	0.69	0.01	0.232	0.001	149
				52	3.5	36		0.4	8.2	0.04	
8d	94.95	0.033	2.55	0.62	0.241	0.80	0.51	0.007	0.298	0.006	155
				31	12	40.6		0.4	15.1	0.3	
8e	92.1	0.004	0.68	2.15	1.56	2.60	0.025	0.02	0.79	0.007	410
			4.6	28.6	21	34.6		0.3	11	0.09	

(a) Measurements for ammonia are for gas phase only and do not include ammonia dissolved in the solid-liquid phase, which will be reported in a subsequent document.

samples was always less than its detection limit. Because traces of other hydrocarbons found in some samples were omitted from Table 6, the sum of all percents for some of the runs are less than 100%.

The relative concentrations of NO_x gases produced in the samples in Table 6 increase at the higher temperatures. This may be of increasing importance for tanks that have a low inventory of total organic carbon (TOC). The NO_x production from SY-103 waste was much less than that of S-102 waste at the same temperatures. The implication is that as the organic concentration decreases (as in Tank S-102) the source for NO_x reduction is also removed, consistent with observations using simulated waste systems (Meisel 1991). Thus waste tanks deficient in organics may have increased NO_x production.

The predicted mole percent composition at each temperature is shown graphically in Figure 3. The data shown in the figure are the predicted mole percent compositions of the major components in gas generated due to thermal processes. The percent nitrogen data in Figure 3 at 80°C and below were determined by extrapolation from the Arrhenius plot of the data at 100 and 120°C (see Section 3.3).

Figure 3 shows that the fraction of hydrogen decreased with increased temperature in the range of 60 to 120°C, the fraction of nitrous oxide decreased slightly, and the fractions of nitrogen and methane increased. The consequences of changes in relative concentrations of gases are seen in differences in activation energies for the production of these gases (see Section 3.3). Using the percent composition data, reaction times, and mass of each sample, rates of gas generation were determined. These rates are given in Table 7 as a function of temperature.

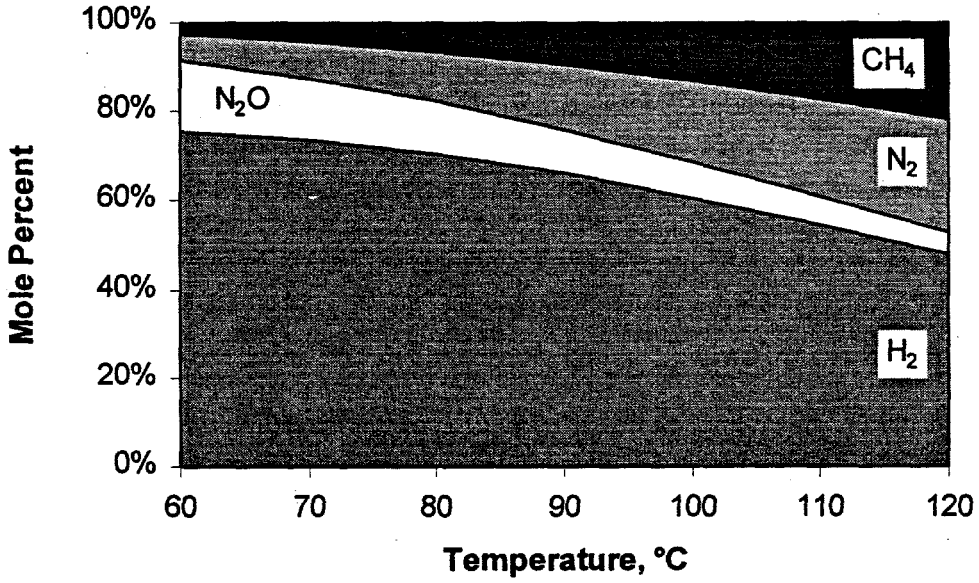

Figure 3. Predicted Mole Percent Composition of Major Components in Gas Generated at Various Temperatures Due to Thermal Processes

Table 7. Gas Generation Rates from Thermal Treatment of Tank S-102 Waste (no external radiation source was used for these samples)

60°C Gas Generation Rates, mol/kg/day

Run	N_2[a]	N_2O	H_2	NH_3[b]	NO_x	CH_4	$C_2H_{2,4,or\,6}$	Other HC[c]	Total
1a	5.6E-6	3.7E-7	1.3E-6						1.7E-6
1b	3.0E-6	1.4E-7	1.1E-6						1.2E-6
1c	2.1E-6	1.2E-7	6.6E-7						7.9E-7
2a	8.2E-6	6.2E-7	2.6E-6			8.1E-8			3.3E-6
2b	3.9E-6	3.3E-7	1.8E-6			7.0E-8			2.2E-6
2c	1.5E-6	2.6E-7	1.7E-6			7.1E-8			2.0E-6

80°C Gas Generation Rates, mol/kg/day

Run	N_2[a]	N_2O	H_2	NH_3[b]	NO_x	CH_4	$C_2H_{2,4,or\,6}$	Other HC[c]	Total
3a	3.1E-4	2.6E-6	5.1E-6			3.4E-7			8.0E-6
3b	1.1E-5	1.2E-6	5.6E-6		2.9E-7	4.8E-7			7.6E-6
3c	5.5E-6	9.7E-7	7.0E-6		1.2E-6	6.5E-7		3E-7	1.0E-5
4a	2.3E-4	2.8E-6	6.4E-6			5.7E-7			9.8E-6
4b	1.0E-5	1.3E-6	6.5E-6			7.1E-7			8.5E-6
4c	4.1E-6	1.2E-6	7.3E-6	8.6E-7	5.7E-7	8.9E-7		3E-7	1.1E-5

100°C Gas Generation Rates, mol/kg/day

Run	N_2[a]	N_2O	H_2	NH_3[b]	NO_x	CH_4	$C_2H_{2,4,or\,6}$	Other HC[c]	Total
5a	7.0E-4	1.2E-5	2.0E-5			3.2E-6			3.5E-5
5b	1.7E-4	1.9E-6	2.1E-5			4.2E-6			2.7E-5
5c	1.4E-5	2.0E-6	2.6E-5	1.3E-7	3.2E-7	5.9E-6			3.5E-5
5d	4.2E-6	1.7E-6	2.7E-5		6.2E-7	7.4E-6		1E-6	3.8E-5
6a	2.1E-3	1.2E-5	3.0E-5			6.0E-6			4.7E-5
6b	1.6E-4	3.5E-6	2.4E-5		3.7E-6	5.7E-6			3.7E-5
6c	1.1E-5	3.2E-6	1.7E-5		3.8E-6	4.3E-6			2.8E-5
6d	4.8E-6	2.5E-6	3.0E-5		1.2E-6	9.2E-6		1E-6	4.4E-5

120°C Gas Generation Rates, mol/kg/day

Run	N_2[a]	N_2O	H_2	NH_3[b]	NO_x	CH_4	$C_2H_{2,4,or\,6}$	Other HC[c]	Total
7a	1.1E-3	6.6E-5	2.3E-4	1.0E-5		1.2E-4	5E-6	5E-6	4.3E-4
7b	6.0E-4	1.3E-5	2.1E-4		1.6E-6	9.8E-5	2E-7		3.2E-4
7c	2.0E-4	1.0E-5	1.4E-4		4.2E-6	9.8E-5		5E-7	2.5E-4
7d	7.6E-5	3.2E-5	8.3E-5	5.4E-7	1.6E-5	8.9E-5	3E-7		2.2E-4
7e	4.3E-5	7.7E-5	7.6E-5	6.3E-7	1.1E-5	7.9E-5	2E-7	3E-4	5.4E-4
8a	1.4E-3	5.6E-5	1.2E-4	3.2E-6		4.1E-5	3E-6	3E-6	2.2E-4
8b	8.4E-4	1.7E-5	1.9E-4	7.5E-7	3.5E-6	8.1E-5	2E-7		3.0E-4
8c	2.5E-4	8.8E-6	1.3E-4	8.9E-7	2.1E-5	9.1E-5	9E-8	4E-7	2.5E-4
8d	2.1E-4	2.0E-5	5.2E-5	5.8E-7	2.5E-5	6.7E-5	5E-7		1.6E-4
8e	2.2E-5	5.1E-5	7.0E-5	6.5E-7	2.6E-5	8.5E-5	2E-7	2E-4	5.0E-4

(a) The nitrogen rates are uncorrected for atmospheric contamination, except for runs 7e and 8e.
(b) Measurements for ammonia are for gas phase only and do not include ammonia dissolved in the solid-liquid phase, which will be reported in a subsequent document.
(c) Hydrocarbons.

3.1.2 Radiolytic Gas Generation from Tank S-102 Waste

This section contains the data from gases produced radiolytically by placing a ^{137}Cs source (gamma capsule) next to the reaction vessels while heating the material in the reaction vessels to the same temperatures used in the thermal-only experiments (60, 80, 100, and 120°C). The radiolytic reactions were run in duplicate at each temperature. For each reaction, fresh S-102 material was placed into a separate reaction vessel (see Table 2). For each reaction vessel, three to five samples of the generated gases were taken during the course of each reaction sequence. Gas generation rates were determined from the heating time, percent composition of the gas, total moles of gas in each system when the sample was taken (Table 8), and from the mass of tank material present in each reaction vessel (Table 2). The time each vessel was heated between sampling events is given in Tables 8 and 9. In these tables, the individual runs are identified by a number and letter. The number identifies the reaction vessel, and the letter identifies the gas sampling event. For example, entries for runs 9a and 10a give data at the first gas sampling event for radiolytic reaction vessels 9 and 10, which are duplicates at 60°C.

The mole percent composition of the gas sampled at the end of each run is given in Table 9. Of more interest is the composition of gas generated, which is presented below the entry for each run and shaded gray. These values were corrected for air as in the thermal measurements above.

Using the percent composition data, reaction times, and mass of each sample, rates of gas generation under radiolytic conditions were determined. These rates are given in Table 10 as a function of temperature.

Table 8. Total Moles of Gas Present in Each Radiolytic Gas Generation Reaction System When Gas Samples Were Taken

Run	Time, hr	60°C	Run	Time, hr	80°C	Run	Time, hr	100°C	Run	Time, hr	120°C
9a	458	0.0562	11a	458	0.0518	13a	114	0.0571	15a	114	0.0588
9b	429	0.0579	11b	429	0.0560	13b	160	0.0536	15b	161	0.0566
9c	529	0.0560	11c	529	0.0550	13c	160	0.0529	15c	161	0.0551
10a	458	0.0531	12a	458	0.0549	14a	113	0.0559	16a	115	0.0548
10b	429	0.0546	12b	429	0.0592	14b	161	0.0536	16b	161	0.0532
10c	529	0.0525	12c	529	0.0526	14c	161	0.0525	16c	161	0.0512

Table 9. Percent Composition of Gas Sampled from Radiolytic Experiments (including helium) and Gas Formed (shaded), and Heating Times for Duplicate Systems at Four Temperatures (an external ^{137}Cs gamma source [37,000 R/h] was added to these waste samples during gas generation)

	Mole Percent of Gas Formed at 60°C										
Run	He	Ar	N_2	H_2	N_2O	CH_4	O_2	NH_3[(a)]	NO_x	$C_2H_{2,4,or\,6}$	Time, hr
9a	98.4	0.006	0.59	0.53	0.324	0.016	0.114		0.008		458
			23	47	28.6	1.4			0.7		
9b	96.40	0.028	2.52	0.49	0.42	0.018	0.101		0.02		429
			27	38	32	1.4			2		
9c	98.3	0.005	0.62	0.46	0.56	0.019	0.051		0.02	0.004	529
			26	32	39	1.3			1	0.3	
10a	98.4	0.005	0.52	0.55	0.38	0.018	0.094		0.03	0.002	458
			22	44	30.4	1.4			2.4	0.2	
10b	96.85	0.022	2.02	0.48	0.45	0.018	0.110		0.04	0.005	429
			26	36	34	1.3			3	0.4	
10c	98.2	0.005	0.61	0.51	0.55	0.018	0.075	0.02	0.05	0.005	529
			24	34	36	1.2		1	3	0.3	

	Mole Percent of Gas Formed at 80°C										
Run	He	Ar	N_2	H_2	N_2O	CH_4	O_2	NH_3[(a)]	NO_x	$C_2H_{2,4,or\,6}$	Time, hr
11a	97.8	0.005	0.93	0.89	0.279	0.037	0.051			0.003	458
			36	47	14.7	2.0				0.2	
11b	96.59	0.017	1.88	1.01	0.348	0.056	0.096			0.006	429
			30	49	17	2.7				0.3	
11c	98.2	0.005	0.57	0.69	0.249	0.038	0.037	0.2	0.002	0.006	529
			21	46	17	2.5		13	0.1	0.4	
12a	97.4	0.013	1.19	0.86	0.323	0.054	0.101		0.008	0.001	458
			18	56	21.2	3.5			0.5	0.07	
12b	96.97	0.019	1.72	0.84	0.291	0.053	0.085			0.007	429
			19	55	19	3.4				0.5	
12c	98.3	0.006	0.57	0.67	0.249	0.052	0.070	0.1	0.01	0.006	529
			18	51	19	3.9		8	1	0.5	

(a) Measurements for ammonia are for gas phase only and do not include ammonia dissolved in the solid-liquid phase, which will be reported in a subsequent document.

3.2 Thermal and Radiolytic Rate Parameters for Gas Generation from Tank S-102 Waste

The three most important mechanisms for gas generation from waste have been determined to be 1) radiolytic decomposition of water and some organic species; 2) thermally driven chemical reactions, mainly involving organic complexants and solvents; and 3) chemical decomposition of the steel tank walls (Johnson et al. 1997). The total gas generation rate is the sum of the radiolytic, thermal, and corrosion rates:

$$\text{Total Rate} = \text{Radiolytic Rate} + \text{Thermal Rate} + \text{Corrosion Rate} \quad (1)$$

Table 9 (contd)

Mole Percent of Gas Formed at 100°C

Run	He	Ar	N_2	H_2	N_2O	CH_4	O_2	NH_3[(a)]	NO_x	$C_2H_{2,4,or\,6}$	Time, hr
13a	98.19	0.023	0.93	0.65	0.100	0.051	0.037		0.009		114
				80	12.3	6.3			1.1		
13b	97.6	0.009	0.74	1.20	0.217	0.110	0.047		0.088		160
			9	68	12	6.2			5.0		
13c	98.4	0.005	0.342	0.84	0.174	0.096	0.047		0.07	0.001	160
			7	66	14	7.5			5	0.08	
14a	98.68	0.003	0.57	0.51	0.129	0.060	0.045			0.004	113
			41	43	10.8	5.0				0.3	
14b	97.8	0.004	0.60	1.19	0.195	0.133	0.063			0.002	161
			22	61	10	6.8				0.1	
14c	98.4	0.002	0.339	0.92	0.157	0.16	0.035			0.002	161
			21	58	10	10				0.13	

Mole Percent of Gas Formed at 120°C

Run	He	Ar	N_2	H_2	N_2O	CH_4	O_2	NH_3[(a)]	NO_x	$C_2H_{2,4,or\,6}$	Time, hr
15a	94.7	0.010	1.93	2.15	0.252	0.82	0.053	0.006		0.009	114
			28	48	5.60	18		0.1		0.2	
15b	95.0	0.005	0.67	2.66	0.172	1.43	0.063	0.02			161
			9	56	4	30		0.4			
15c	97.0	0.003	0.356	1.32	0.102	1.13	0.051		0.012		161
			10	46	3.6	40	~0.6		0.4		
16a	94.1	0.007	1.70	2.36	0.281	1.15	0.092	0.2	0.013	0.016	115
			24	45	5.30	22		4	0.25	0.3	
16b	94.6	0.003	0.47	2.67	0.184	1.89	0.045	0.09	0.009	0.002	161
			7	51	4	36		1.7	0.17	0.04	
16c	96.6	0.003	0.366	1.38	0.146	1.46	0.047		0.026	0.002	161
			9	42	4.4	44			0.8	0.06	

(a) Measurements for ammonia are for gas phase only and do not include ammonia dissolved in the solid-liquid phase, which will be reported in a subsequent document.

Because radiolytic and thermal rates dominate (Johnson et al. 1997), they are the focus of these experiments. The thermal rate varies with temperature. The relation between thermal rates at different temperatures is given by the Arrhenius equation:

$$k = Ae^{\left(\frac{-E_a}{RT}\right)} \tag{2}$$

where R is the gas constant, 8.314 J/K-mol, and T is temperature in Kelvin. Values of activation energy, E_a, and pre-exponential factor, A, can be determined from the rates measured in the reaction vessels. The equation will allow the thermal rate of gas generation to be calculated at tank temperature, where the rate is so slow that it would be difficult to measure directly.

Initial rates of reaction must be known to determine E_a and A from equation 2. The rates of nitrous oxide and methane generation did not decrease significantly with time, so the initial rates for these gases were taken to be the average of all runs at a given temperature. The rates of

Table 10. Radiolytic Gas Generation Rates from Tank S-102 (an external ^{137}Cs gamma source [37,000 R/h] was added to these waste samples during gas generation)

60° Gas Generation Rates, mol/kg/day

Run	N_2	N_2O	H_2	NH_3[(a)]	NO_x	CH_4	$C_2H_{2,4,or\,6}$	Other HC[(b)]	Total
9a	7.5E-6	9.5E-6	1.6E-5		2.4E-7	4.7E-7			3.3E-5
9b	1.1E-5	1.4E-5	1.6E-5		6.5E-7	5.8E-7			4.2E-5
9c	9.4E-6	1.4E-5	1.2E-5		5.1E-7	4.8E-7	1.0E-7		3.6E-5
10a	7.5E-6	1.1E-5	1.5E-5		8.3E-7	5.0E-7	5.6E-8		3.5E-5
10b	1.1E-5	1.4E-5	1.5E-5		1.2E-6	5.5E-7	1.5E-7		4.1E-5
10c	8.5E-6	1.3E-5	1.2E-5	4.8E-7	1.2E-6	4.3E-7	1.2E-7		3.6E-5

80° Gas Generation Rates, mol/kg/day

Run	N_2	N_2O	H_2	NH_3[(a)]	NO_x	CH_4	$C_2H_{2,4,or\,6}$	Other HC[(b)]	Total
11a	1.8E-5	7.6E-6	2.4E-5			1.0E-6	8.1E-8		5.1E-5
11b	2.0E-5	1.1E-5	3.2E-5			1.8E-6	1.9E-7	6.3E-7	6.5E-5
11c	8.0E-6	6.2E-6	1.7E-5	5.0E-6	5.0E-8	9.5E-7	1.5E-7		3.7E-5
12a	7.8E-6	9.3E-6	2.5E-5		2.3E-7	1.6E-6	2.9E-8		4.4E-5
12b	9.9E-6	9.6E-6	2.8E-5			1.8E-6	2.3E-7	1.7E-6	5.1E-5
12c	5.6E-6	5.9E-6	1.6E-5	2.4E-6	2.4E-7	1.2E-6	1.4E-7		3.2E-5

100° Gas Generation Rates, mol/kg/day

Run	N_2	N_2O	H_2	NH_3[(a)]	NO_x	CH_4	$C_2H_{2,4,or\,6}$	Other HC[(b)]	Total
13a		1.2E-5	7.8E-5		1.1E-6	6.1E-6			9.7E-5
13b	1.2E-5	1.7E-5	9.6E-5		7.1E-6	8.8E-6		4.0E-7	1.4E-4
13c	7.2E-6	1.4E-5	6.6E-5		5.5E-6	7.6E-6	7.9E-8	4.0E-7	1.0E-4
14a	5.8E-5	1.5E-5	6.1E-5			7.1E-6	4.8E-7		1.4E-4
14b	3.5E-5	1.6E-5	9.5E-5			1.1E-5	1.6E-7	4.0E-7	1.6E-4
14c	2.7E-5	1.2E-5	7.2E-5			1.3E-5	1.6E-7	7.8E-8	1.2E-4

120° Gas Generation Rates, mol/kg/day

Run	N_2	N_2O	H_2	NH_3[(a)]	NO_x	CH_4	$C_2H_{2,4,or\,6}$	Other HC[(b)]	TOTAL
15a	1.6E-4	3.1E-5	2.7E-4	7.4E-7		1.0E-4	1.1E-6		5.6E-4
15b	3.5E-5	1.5E-5	2.2E-4	1.7E-6		1.2E-4		1.0E-6	4.0E-4
15c	2.2E-5	8.4E-6	1.1E-4		9.9E-7	9.3E-5		8.2E-7	2.3E-4
16a	1.5E-4	3.2E-5	2.7E-4	2.3E-5	1.5E-6	1.3E-4	1.8E-6		6.0E-4
16b	3.1E-5	1.5E-5	2.1E-4	7.1E-6	7.1E-7	1.5E-4	1.6E-7	1.0E-6	4.2E-4
16c	2.2E-5	1.1E-5	1.1E-4		2.0E-6	1.1E-4	1.5E-7	9.2E-7	2.5E-4

(a) Measurements for ammonia are for gas phase only and do not include ammonia dissolved in the solid-liquid phase, which will be reported in a subsequent document.
(b) Hydrocarbons.

hydrogen and nitrogen generation decreased with time at higher temperatures. The decrease was modeled by a first-order rate law: $Rate = k[c]$. The observed rates are fit to thermal rates calculated with the following equation:

$$calculated\ \ rate = \frac{c_i\left(-e^{-time_f \times k} + e^{-time_i \times k}\right)}{time_f - time_i} \qquad (3)$$

where c_i represents the initial concentration of some component(s) that is consumed with time. The initial rate is $k \times c_i$. Consideration of more complicated rate laws was not warranted.

The radiolytic rate in equation 1 was assumed to be temperature-independent based on observations that the rates for water radiolysis are nearly temperature-independent; also, radiolytic rates in SY-103 were observed to be temperature-independent. Radiolytic rates are given by

$$\text{Radiolytic rate (mol/kg/day)} = \text{G-value(molecules/100 eV)} \times \text{dose-rate (R/hr)} / 4.02\text{E}7 \quad (4)$$

In practice, equations 1–4 were combined into one. The parameters in that equation were determined by nonlinear least squares using the Marquardt-Levenberg algorithm (Marquardt 1963). For each gas, the rate parameters E_a, A, G-value, and, for hydrogen and nitrogen, c_i, were determined using all the rate data. The entire data set (thermal and radiolytic) was fit simultaneously using equations 1–4. For each gas, a three- or four-parameter model described all the rate data, both thermal and radiolytic.

The rate parameters determined for each gas are given in Table 11. Both A and its natural logarithm are given. The 95% confidence interval for a value in the table is the value plus or minus the number in parentheses. The large R^2 values given in the table support the assumption that G-values are mainly temperature-independent. The goodness of fit was not improved by allowing the G-values to vary as a function of temperature, and they are therefore accepted as constant. R^2 is the correlation coefficient, a measure of the goodness of the least squares fit. The small R^2 value for nitrogen is due to uncertainty in the correction for atmospheric contamination.

A represents the pre-exponential factor for a zero-order rate law. For gases following first-order kinetics, A is the product of c_i and a first-order A, $A_{first\ order}$. The values for hydrogen of $A_{first\ order}$ and c_i are 5.2E+10 mol/kg/day/molar and 0.004(± 0.002) molar. The values for nitrogen are 5E+15 mol/kg/day/molar and 0.0010(± 0.0003) molar. An Arrhenius plot of the gas generation rates for hydrogen, nitrous oxide, and methane, along with activation energies, is shown in Figure 4.

The predicted rates (from equations 1 through 4) for hydrogen gas generation are plotted with the observed rates for the thermal (with self radiolysis) and radiolytic rate data in Figure 5. All the experimental data (thermal and radiolytic) for hydrogen generation are included in this figure. Plots of the thermal and radiolytic gas generation data for nitrous oxide, nitrogen, and methane are displayed with the calculated (predicted) rates in Figures 6 through 8, respectively.

Table 11. Thermal and Radiolytic Rate Parameters for Gas Generation from S-102 Waste

	H_2	N_2O	N_2	CH_4
E_a, kJ/mol	91(±7)	79(±11)	127(±70)	137(±7)
A, mol/kg/day	2.1E+8	5.6E+5	5.0E+12	1.1E+14
ln(A)	19(±3)	13(±4)	29(±22)	32(±2)
G-value	0.017(±0.004)	0.009(±0.003)	0.010(±0.003)	0.0005(±0.0002)
R^2	0.946	0.841	0.70	0.975

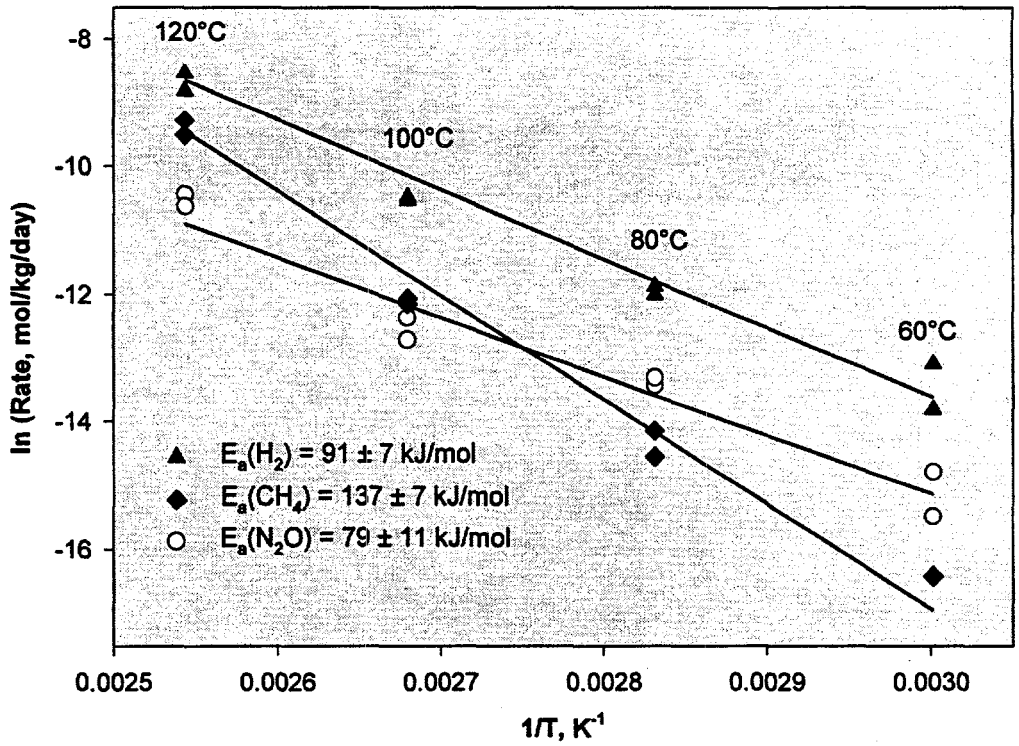

Figure 4. Comparison of Gas Generation Rates in Tank S-102 (nitrogen is omitted)

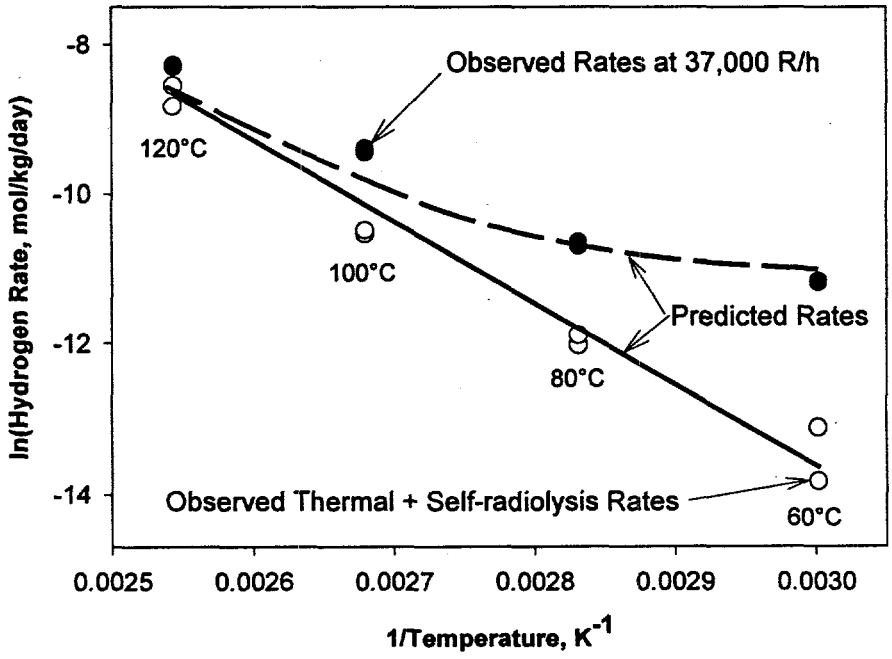

Figure 5. Observed and Predicted Hydrogen Generation Rates Under Thermal and Radiolytic Conditions (rate data are taken from Tables 7 and 10)

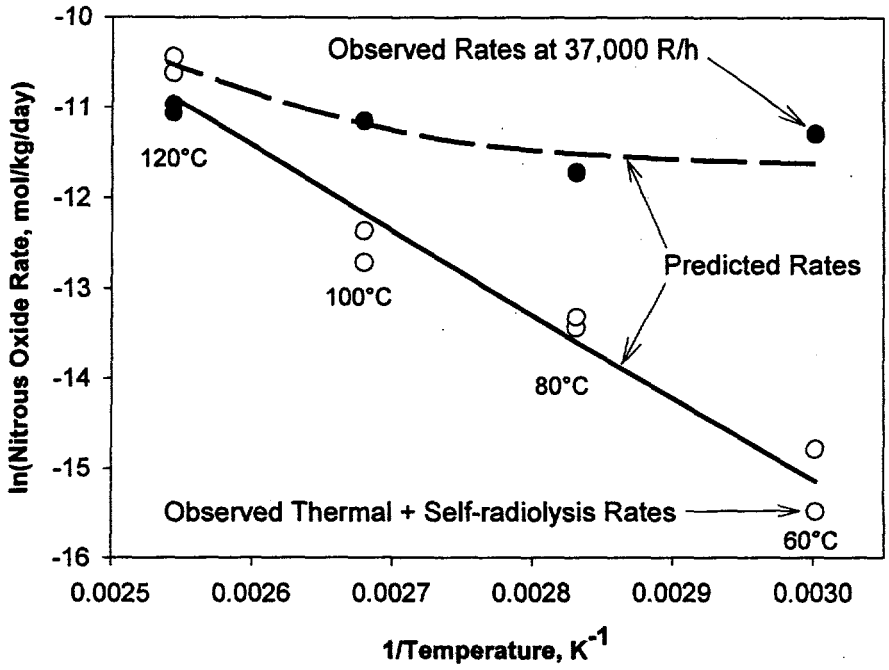

Figure 6. Observed and Predicted Nitrous Oxide Generation Rates Under Thermal and Radiolytic Conditions (rate data are taken from Tables 7 and 10)

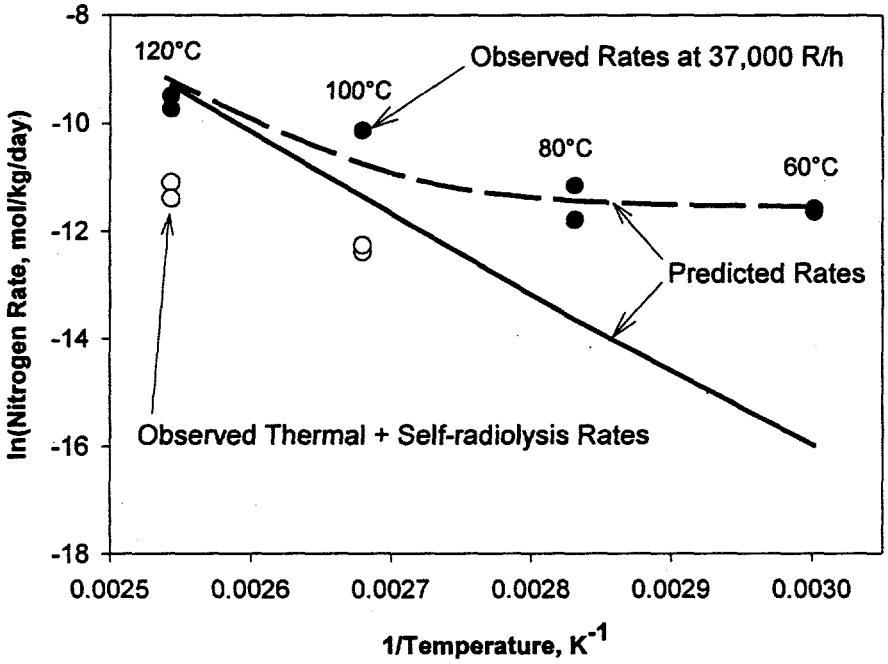

Figure 7. Observed and Predicted Nitrogen Generation Rates Under Thermal and Radiolytic Conditions (rate data are taken from Tables 7 and 10)

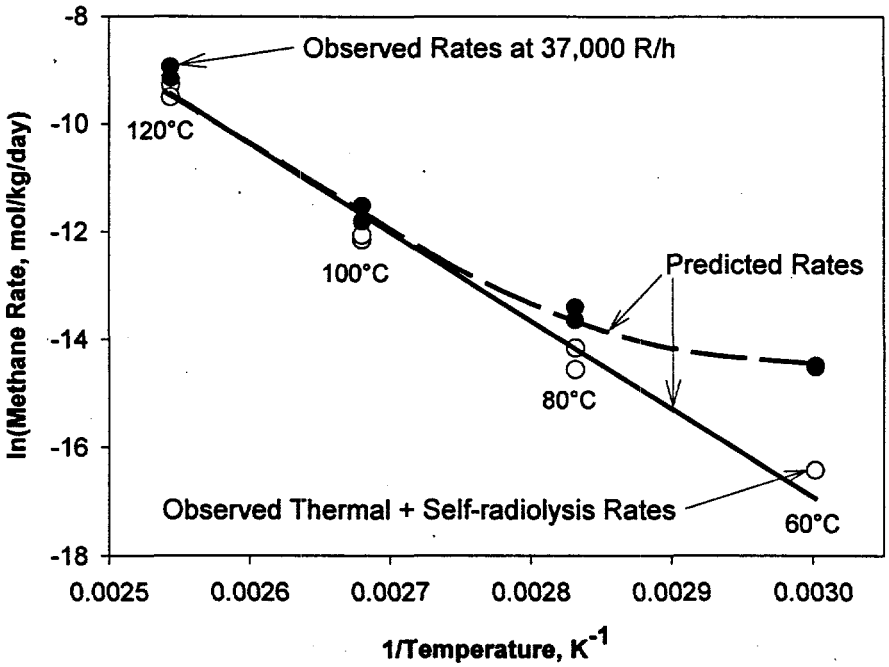

Figure 8. Observed and Predicted Methane Generation Rates Under Thermal and Radiolytic Conditions (rate data are taken from Tables 7 and 10)

Tank S-102 has an average temperature of approximately 41°C and an average dose rate of 207 R/hr (see Section 2.3). The predicted rates of gas generation under these conditions, calculated using the parameters in Table 11, are given in Table 12. The uncertainty in the percent composition (Table 12) is largely due to the uncertainty in nitrogen generation rates. The rates have also been separated into thermal and radiolytic components.

Using the measured thermal and radiolytic activation parameters (from Table 11), the predicted rates for hydrogen generation under tank conditions (207 R/hr) and variable temperatures were calculated below and above the average temperature (41°C) for S-102. These values are displayed in Figure 9 for hydrogen gas generation. Due to variability in the temperature of the waste in S-102 as a function of depth, a display of the predicted gas generation rate as a function of temperature was deemed useful. The 95% confidence interval is also displayed in the plot. Similar plots were prepared for nitrous oxide, nitrogen, and methane and are shown in Figures 10 through 12, respectively. The confidence interval for the predicted nitrogen values ballooned above ~45°C due the lack of thermal data below 100°C for input into the model.

Factors that are bulk averages of tank parameters may influence the calculated gas generation rates. Parameters that were bulk-averaged include density, elemental analysis, radionuclide inventory, and temperature. The variability of these analyses will not affect the measured gas generation from our tests. The G-values and activation energies determined experimentally do not depend on the values of these analyses since the temperature and dose rate in these gas

Table 12. Gas Generation at Tank Conditions (207 R/h, 41°C) (rates are in mol/kg/day)

	Total Rate	Composition, mol%	Rate Components			
			Radiolytic	Thermal	% Radiolytic	% Thermal
H_2	2.5(±0.6)E-7	61(±11)	8.6E-8	1.6E-7	35	65
N_2O	9(±0.3)E-8	23(±8)	4.8E-8	4.3E-8	53	47
N_2	6(±0.3)E-8	15(±7)	5.3E-8	5.7E-9	90	10
CH_4	5(±0.1)E-9	1.2(±0.5)	2.7E-9	2.2E-9	56	44

generation tests were well controlled. However, the calculation of the gas generation rates under tank conditions using these measured parameters will particularly depend on the accuracy of the radionuclide inventory and temperature of the waste.

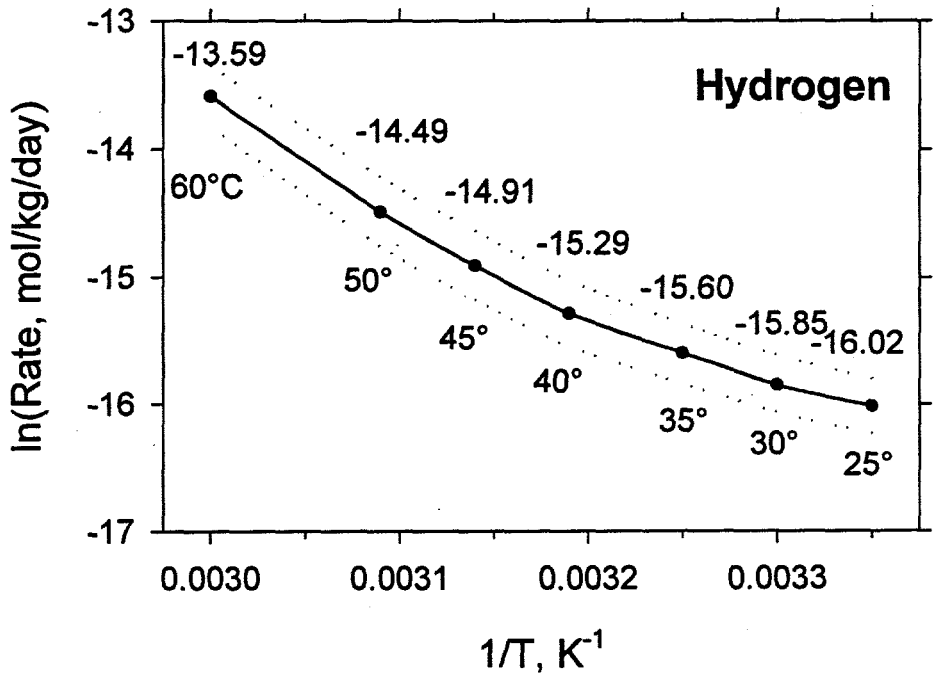

Figure 9. Predicted Rate of Hydrogen Gas Generation Under Tank Conditions (dotted line represents 95% confidence interval for the predicted values)

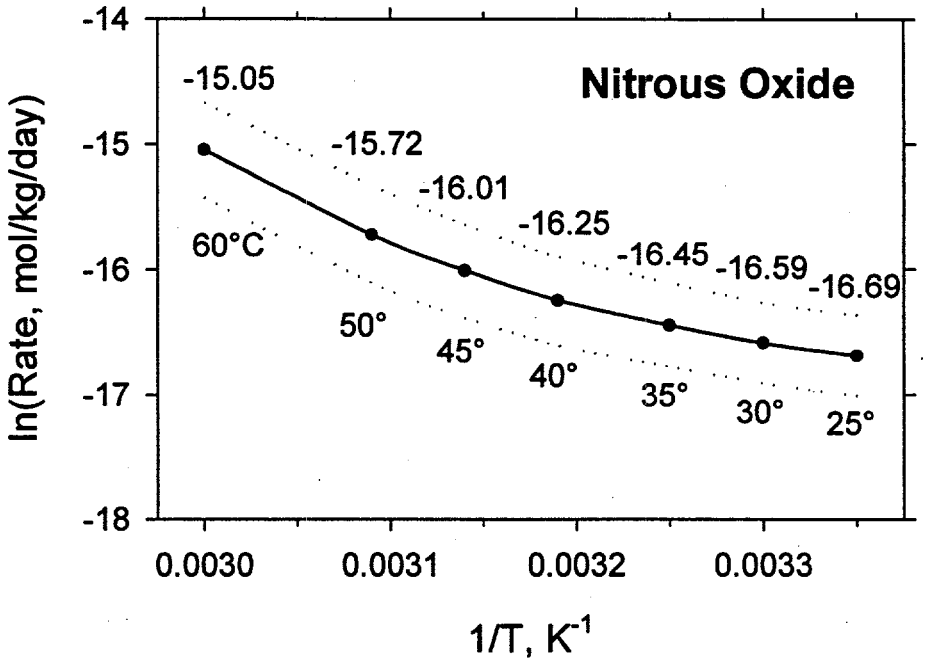

Figure 10. Predicted Rate of Nitrous Oxide Generation Under Tank Conditions (dotted line represents 95% confidence interval for the predicted values)

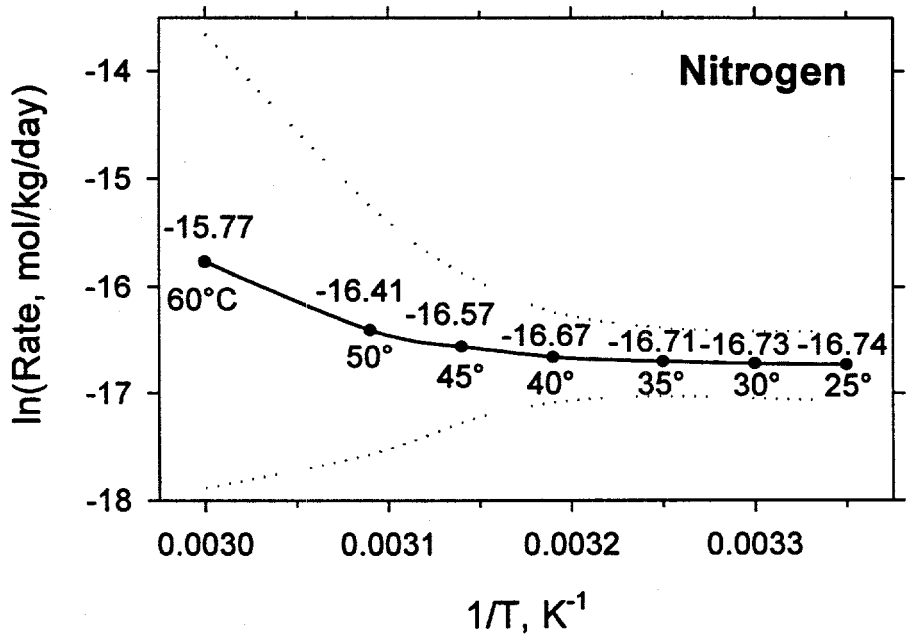

Figure 11. Predicted Rate of Nitrogen Gas Generation Under Tank Conditions (dotted line represents 95% confidence interval for the predicted values)

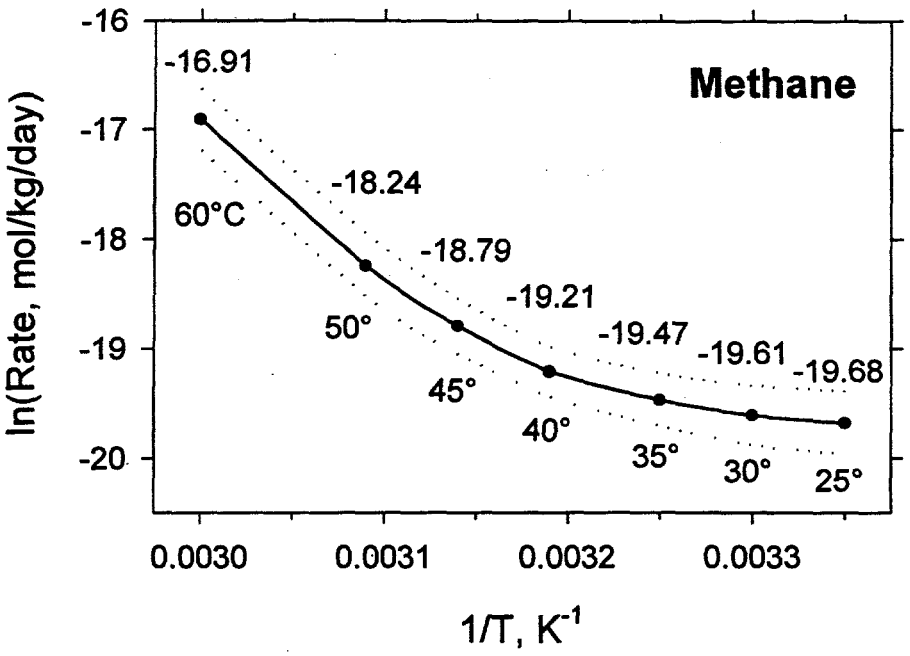

Figure 12. Predicted Rate of Methane Generation Under Tank Conditions (dotted line represents 95% confidence interval for the predicted values)

3.3 Comparison of Gas Generation Rates from S-102 and SY-103 Wastes

In Table 13, thermal activation energies for the major components in Tank S-102 are compared with those obtained previously from Tank SY-103 (Bryan et al. 1996). The radiolytic G-values from gas generation from S-102 and SY-103 wastes are compared in Table 14.

The thermal rate of hydrogen generation in S-102 waste is about a factor of 10 less than that from SY-103 waste. The radiolytic rate for hydrogen generation is lower as well; the value of $G(H_2)$ from S-102 waste is measured as 0.017 molecules/100 eV (Table 14), which is an order of magnitude smaller than the 0.14 molecules/100 eV for SY-103 waste (Bryan et al. 1996).

The lower hydrogen gas generation rates from S-102 material can be partially accounted for by the fact that S-102 waste contains less liquid phase than SY-103 waste. Studies using waste simulants have found that gas generation occurs predominately in the liquid phase rather than in the solid phase (Bryan and Pederson 1995). Gas generation tests on SY-103 waste used samples from the supernatant layer that contained 48.4 wt% water, while the gas generation tests on S-102 waste (this study) used a whole-tank homogenized saltcake containing 27.4 wt% water (Fritts 1996). A comparison of the G-values and pertinent wt% water and TOC data for hydrogen generation from S-102 and SY-103 wastes is included in Table 15.

The lower gas generation rates from Tank S-102 material can also be explained by the fact that S-102 waste contains less total organic carbon (TOC) than SY-103 waste. In simulated waste studies, the role of organics on thermal hydrogen (and nitrogen and nitrous oxide) gas

Table 13. Comparison of Thermal Activation Parameters for Gas Generation from Tank S-102 and SY-103 Wastes

Pre-Exponential Factors (mol/kg/d) and Energies of Activation (kJ/mol)		
Gas	**Tank S-102**	**Tank SY-103**
H_2	E_a = 91 ± 7 A = 2.1E+8	E_a = 91 ± 9 A = 1.4E+9
N_2O	E_a = 79 ± 11 A = 5.6E+5	E_a = 117 ± 9 A = 5.5E+12
N_2	E_a = 127 ± 70 A = 5.0E+12	E_a = 84 ± 10 A = 1.1E+8
CH_4	E_a = 137 ± 7 A = 1.1E+14	E_a = 127 ± 33 A = 4E+14

Table 14. Comparison of Radiolytic G-values for Gas Generation from Tank S-102 and SY-103 Wastes

G-values (molecules/100 eV)		
Gas	**Tank S-102**	**Tank SY-103**
H_2	0.017 ± 0.004	0.14 ± 0.02
N_2O	0.009 ± 0.003	0.033 ± 0.009
N_2	0.010 ± 0.003	0.011 ± 0.006
CH_4	0.0005 ± 0.0002	0.003 ± 0.001

Table 15. Comparison of G-values for Hydrogen Gas Generation from Tanks S-102 and SY-103

	Tank S-102 Composite	**Tank SY-103 Convective layer**
$G(H_2)$, molecules/100 eV	0.017	0.14
TOC, wt%	0.4% (high oxalate)	0.74% (low oxalate)
H_2O content, wt%	27.4%	48.4%

generation has been described in a first-order relationship (Delegard 1980; Bryan et al. 1992, 1995; Pederson and Bryan 1996). For the radiolytic experiments, the lower $G(H_2)$ for S-102 compared with SY-103 waste is consistent with the relationship proposed by Miesel (1991) in which the $G(H_2)$ increases linearly as a function of total C-H (or N-H) bond density. The TOC value for SY-103 has been reported as 0.74% (Pederson and Bryan 1996), with a high fraction

of measured organics as chelator or chelator fragments, rich in C-H and N-H bond density. Preliminary organic analysis of S-102 indicates that greater than half of the 0.4 wt% TOC is oxalate (Carlson 1997) and is not expected to enter into active radiolytic hydrogen generation reactions.

Using the thermal and radiolytic activation parameters for gas generation in actual tank waste, the rate of hydrogen generation in the entire tank can be estimated for Tank S-102. The rate of hydrogen generation in tank material is the sum of thermal and radiolytic rates.

The thermal rate at 41°C is 8.6E-8 mol/kg/day. The radiolytic rate is 1.6E-7 mol/kg/day using a $G(H_2)$ value of 0.017 molecules/100 eV and a tank dose rate of 207 R/hr. The sum of the thermal and radiolytic rates is 2.5E-07 mol/kg/day. Multiplying by the mass of the tank contents, (3.95E+6 kg [Hanlon 1997]) gives a hydrogen generation rate for Tank S-102—from the entire tank—of 1.0 mol/day.

An independent estimate of the rate of hydrogen formation is available.[a] The rate of hydrogen formation in Tank S-102 has been estimated by assuming that the tank generation rate is equal to the amount of hydrogen released from the tank according to the following expression

$$H_2 \text{ rate} = (\text{vent rate}) \times (H_2 \text{ vapor fraction}) \quad (5)$$

where the vent rate was estimated to be 3 cfm (measured from a tracer gas test). The average hydrogen concentration from mass spectroscopy analysis of vapor grab samples was 617 ppm. This gives an estimated hydrogen generation rate of 3 ft^3/day. Assuming this gas is at 25°C and 1 atmosphere gives an observed rate of 3.8 mol H_2/day from the entire tank. The error estimates for the whole-tank hydrogen generation rates were between 100 and 200%.[a] These results are summarized in Table 16 and compared with similar calculations from earlier work using SY-103 waste.

Although the rate of gas generation from tank material at the same temperature is much lower in S-102 than in SY-103, the actual thermal rates for hydrogen production from each tank are similar because the average temperature of S-102 (41°C) is higher than that in SY-103 (31.7°C). The radiolytic rate is dominant over the thermal rate in SY-103. In contrast, the thermal rate dominates in S-102 waste. Since the dose rate in S-102 is about half that in SY-103, and the C-H content is also much less in S-102 than in SY-103, the hydrogen gas generation rate from all sources of S-102 waste is about 10% of that found for SY-103 from the small-scale reaction tests.

The thermal rates of total gas generation for S-102, SY-101, and SY-103 are shown in Figure 13. As can be seen, the rate of total gas generation is lower in S-102 than in Tanks SY-103 and SY-101.

(a) Barton WB. 1997. *Field Estimated Gas Generation Rates.* Presented at Safety Controls by Performance Evaluation (SCOPE) Meeting, April 28–May 2, 1997. Lockheed Martin Hanford Corporation, Richland, Washington.

Table 16. Comparison of Gas Generation Rates in Tanks S-102 and SY-103

	Gas Generation Rate, mol/kg/day			Whole Tank Rate, mol/day	
	Thermal[a]	Radiolytic	Total	This Work	Other
H_2, SY-103 [b]	3.5E-7	1.6E-6	2.0(±0.1)E-6	8.7(±0.4)	10[c]
H_2, S-102	1.6E-7	8.6E-8	2.5(±0.6)E-7	1.0(±0.2)	3.8 (± 4)[d]
N_2O, S-102	5E-8	4E-8	9(±3)E-8	0.4 (± 0.1)	NA[e]
CH_4, S-102	2.7E-9	2.2E-9	5(±1)E-9	0.019 (±0.004)	NA
N_2, S-102	5E-8	6E-9	6(±3)E-8	0.2 (± 0.1)	NA

(a) The temperature of SY-103 is 31.7°C; the temperature of S-102 is 41°C.
(b) Convective layer only (SA Bryan, 1996. *Test Plan: Tank S-102 Gas Generation Testing.* TWSFG97.11, PNNL, Richland, Washington.
(c) Estimated from analysis of vent gases (Wilkins 1995).
(d) Estimated from analysis of vent gases (WB Barton, April 1997. *Field Estimated Gas Generation Rates.* Presented at SCOPE Meeting, Richland, Washington.
(e) Not available.

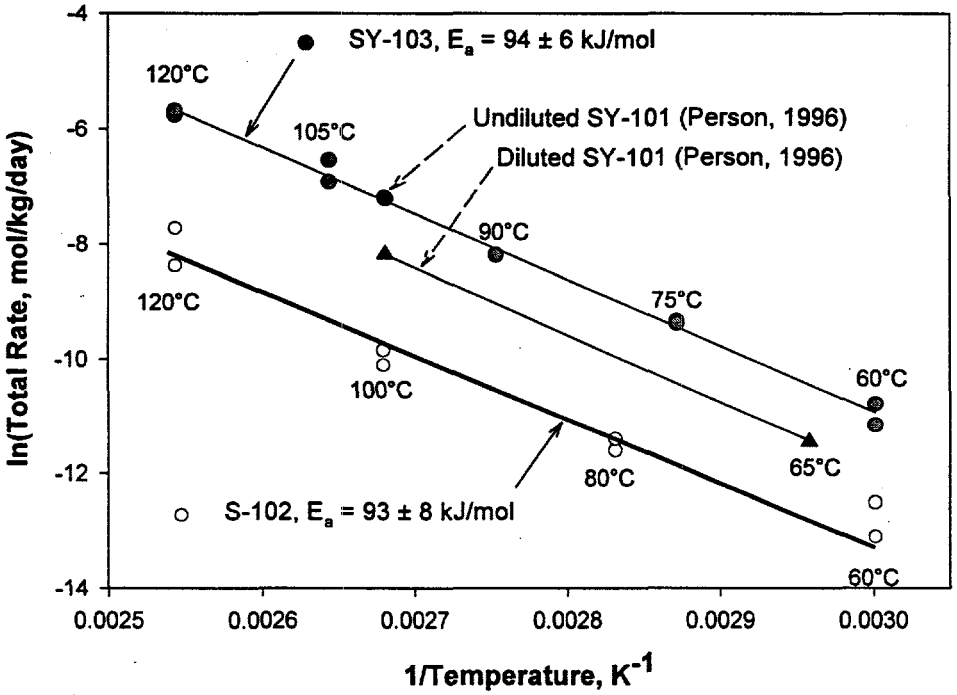

Figure 13. Comparison of Total Gas Generation Rates in S-102, SY-103, and SY-101 Wastes

4.0 Summary

This report summarizes progress made in evaluating mechanisms by which flammable gases are generated in Hanford single-shell tank wastes based on the results of laboratory tests using actual waste from Tank S-102. The waste samples from Tank S-102 used in this study were measured under two conditions: first, with externally applied heat, and second, with externally applied heat and radiation (^{137}Cs capsule).

The main objective of this work is to establish the identity and stoichiometry of degradation products formed in actual tank wastes by thermal and radiolytic processes as a function of temperature. The focus of the gas generation tests on Tank S-102 samples is first on the effect of temperature on the composition and rate of gas generation. Generation rates of nitrogen, nitrous oxide, and hydrogen increased with increased temperature, though at different rates. Thus the composition of the product gas mixture varied with temperature. The fraction of hydrogen decreased with increased temperature in the range 60 to 120°C, the fraction of nitrous oxide decreased slightly, and the fraction of nitrogen and methane increased. The consequences of changes in relative concentrations of gases are seen in differences in activation energies for the production of these gases.

Arrhenius treatment of the rate data revealed activation parameters for gas generation from Tank S-102. Based on the rate of formation of each component gas in the systems, activation energies were calculated. The activation energies (E_a) for formation of these components are 91 ± 7 kJ/mole (95% confidence interval) for H_2, 79 ± 11 kJ/mole for N_2O, 127 ± 70 kJ/mole for N_2, and 137 ± 7 kJ/mol for CH_4.

The second phase of this work is the study of the gas generation capacity of Tank S-102 waste in the presence of a 37,000 rad/hr (^{137}Cs) external gamma source. The radiolytic G-values for gas generation for H_2, N_2O, N_2 and CH_4 are 0.017 (±0.004), 0.009 (±0.003), 0.009 (±0.003), and 0.0005 (±0.0002) molecules/100 eV, respectively.

Using the thermal and radiolytic activation parameters for gas generation in actual tank waste, the rate of hydrogen generation in the entire tank can be estimated for S-102. The rate of hydrogen generation in tank material is a sum of thermal and radiolytic rates. The thermal rate, at 41°C, is 8.6E-8 mol/kg/day. The radiolytic rate is 1.6E-7 mol/kg/day, using a $G(H_2)$ value of 0.017 molecules/100 eV and a tank dose rate of 207 R/hr. The sum of the thermal and radiolytic rates is 2.5E-07 mol/kg/day, which translates to a hydrogen generation rate for the entire tank of 1.0 mol/day.

An independent estimate of the rate of hydrogen formation is available.[a] The rate of hydrogen formation in Tank S-102 has been estimated by assuming that the tank generation rate

---

(a) Barton WB. 1997. *Field Estimated Gas Generation Rates.* Presented at Safety-Controls by Performance Evaluation (SCOPE) Meeting, April 28–May 2, 1997. Lockheed Martin Hanford Corporation, Richland, Washington.

is equal to the amount of hydrogen released from the tank. This gives an estimated hydrogen generation rate of 3 ft^3/day. Assuming this gas is at 25°C and 1 atmosphere gives an observed rate of 3.8 mol H_2/day from the entire tank.

The waste is being analyzed for specific organic components. Separate organic analysis samples were taken before and after heating and radiolysis to help identify the organic species responsible for gas generation. By following the specific organic species present and their concentration changes as a function of heating and irradiation, together with the results of measurements of the gases formed during the heating and irradiation treatments, a better understanding of the organics responsible for gas generation is possible. The organic analysis of the waste will be reported in a subsequent document.

A long-term gas generation test using S-102 waste conducted under thermal and radiolytic conditions that best match the tank waste temperature (43°C) and dose-rate (207 R/h) is being conducted. The results of this experiment will be compared with the predicted gas generation behavior using higher temperatures and dose rates. This experiment is still in progress, and results will be reported in a subsequent gas generation report.

5.0 References

Briesmeister JF. 1993. *Monte Carlo N-Particle Transport Code System.* LA-12625-M, Los Alamos National Laboratory, Los Alamos, New Mexico.

Bryan SA, LR Pederson, RD Scheele, JL Ryan, and JM Tingey. 1992. *Slurry Growth, Gas Retention and Flammable Gas Generation by Hanford Radioactive Waste Tanks: Synthetic Waste Studies.* PNL-8169, Pacific Northwest Laboratory, Richland, Washington.

Bryan SA and LR Pederson. 1994. *Composition, Preparation, and Gas Generation Results from Simulated Wastes of Tank 241-SY-101.* PNL-10075, Pacific Northwest Laboratory, Richland, Washington.

Bryan SA and LR. Pederson. 1995. *Thermal and Combined Thermal and Radiolytic Reactions Involving Nitrous Oxide, Hydrogen, and Nitrogen in the Gas Phase; Comparison of Gas Generation Rates in Supernate and Solid Fractions of Tank 241-SY-101 Simulated Wastes.* PNL-10490, Pacific Northwest Laboratory, Richland, Washington.

Bryan SA, LR Pederson, CM King, SV Forbes, and RL Sell. 1996. *Gas Generation from Tank 241-SY-103 Waste.* PNL-10978, Pacific Northwest Laboratory, Richland, Washington.

Campbell JA, S Clauss, KA Grant, FV Hoopes, BD Lerner, RB Lucke, GM Mong, JK Rau, KL Wahl, and RT Steele. 1994. *Flammable Gas Safety Program Analytical Methods Development.* PNL-10127, Pacific Northwest Laboratory, Richland, Washington.

Carlson CD. 1997. *Speciation of Organic Carbon in Hanford Waste Storage Tanks: Part 1.* PNNL-11480, Pacific Northwest National Laboratory, Richland, Washington.

Delegard C. 1980. *Laboratory Studies of Complexed Waste Slurry Volume Growth in Tank 241-SY-101.* RHO-LD-124, Rockwell Hanford Operations, Richland, Washington.

Eggers RF. 1996. *Tank Characterization Report for Single-Shell Tank S-102.* WHC-SD-WM-ER-611, Westinghouse Hanford Company, Richland, Washington.

Fritts LL. 1996. *Final Report for Tank S-102 Push Mode Cores 125 and 130.* WHC-SD-WM-DP-179 Rev. 1, Westinghouse Hanford Company, Richland, Washington.

Hanlon BM. 1997. *Waste Tank Summary Report for Month Ending April 30, 1997.* HNF-EP-0182-109, Lockheed Martin Hanford Corp., Richland, Washington.

Johnson GD, WB Barton, RC Hill, JW Brothers, SA Bryan, PA Gauglitz, LR Pederson, CW Stewart, and LH Stock. 1997. *Flammable Gas Project Topical Report.* HNF-SP-1193 Rev. 2, Project Hanford Management Contractor, Richland, Washington.

Kocher DC. 1981. *Radioactive Decay Data Tables.* DOE/TIC-11026, Health and Safety Research Division, Oak Ridge National Laboratory. U.S. DOE, Washington, DC.

Laidler KJ. 1987. *Chemical Kinetics, 3rd Ed.* Harper and Row, New York.

Marquardt DW. 1963. "An Algorithm for Least Squares Estimation of Parameters." *Journal of the Society of Industrial and Applied Mathematics*, 11:431-441.

Meisel D, H Diamond, EP Horowitz, CD Jonah, MS Matheson, MC Sauer Jr., and JC Sullivan. 1991. *Radiation Chemistry of Synthetic Waste.* ANL-91/40, Argonne National Laboratory, Argonne, Illinois.

Pederson LR and SA Bryan. 1996. *Status and Integration of Studies of Gas Generation in Hanford Wastes.* PNNL-11297, Pacific Northwest National Laboratory, Richland, Washington.

Person JC. 1996. *Effects of Oxygen Cover gas and NaOH Dilution on Gas Generation in Tank 241-SY-101 Waste.* WHC-SD-WM-DTR-043, Westinghouse Hanford Company, Richland, Washington.

Spinks JTW and RJ Woods. 1990. *An Introduction to Radiation Chemistry.* John Wiley and Sons, New York.

Wilkins NE. 1995. *Tank 241-SY-103 Core Sample: Interpretation of Results.* WHC-SD-WM-TI-712, Westinghouse Hanford Company, Richland, Washington.

Distribution

No. of Copies

Offsite

2 DOE/Office of Scientific and Technical Information

H. Babad
2540 Cordoba Court
Richland, WA 99352

E. K. Barefield
225 North Avenue
Boggs Chemistry Building
Georgia Institute of Technology
Atlanta, GA 30332

D. O. Campbell
102 Windham Road
Oak Ridge, TN 37830

C. W. Forsberg
MS-6495
P.O. Box 2008
Oak Ridge, TN 37831-6495

B. S. Hudson
Lawrence Livermore National Laboratory, L-221
P.O. Box 808
Livermore, CA 94550

L. Kovach
NUCON
P.O. Box 29151
Columbus, OH 43229

T. S. Kress
102-B Newridge Road
Oak Ridge, TN 37830-8118

No. of Copies

T. E. Larson
2711 Walnut St.
Los Alamos, NM 87544

2 Los Alamos National Laboratory
P.O. Box 1664
Los Alamos, NM 87545
Attn: S. Agnew
W. L. Kubic

D. Meisel
Argonne National Laboratory
9700 South Cass Avenue
Argonne, IL 60439

D. A. Powers
Sandia National Laboratories
MS 9744
P.O. Box 5800
Albuquerque, NM 87185-0744

W. W. Schulz
727 Sweetleaf Drive
Wilmington, DE 19808

S. E. Slezak
806 Hermosa NE
Albuquerque, NM 87110

Onsite

2 DOE Richland Operations Office

C. A. Groendyke S7-54
G. W. Rosenwald S7-54

No. of Copies

21 PHMC Team

S. A. Barker	R2-11
G. S. Barney	T5-12
W. B. Barton	R2-12
R. E. Bauer	S7-14
R. J. Cash	S7-14
K. A. Gasper	H6-37
D. L. Herting	T6-07
G. W. Hood	S7-73
T. A. Hu	R2-11
J. R. Jewett	T6-07
G. D. Johnson (3)	S7-14
R. M. Marusich	A3-34
J. C. Person	T6-07
D. A. Reynolds	R2-11
E. R. Siciliano	H0-31
L. M. Stock	S7-14
R. J. Van Vleet	A3-34
J. R. White	S7-15
N. E. Wilkins	R2-12

No. of Copies

44 Pacific Northwest National Laboratory

Z. I. Antoniak	K7-15
S. Q. Bennett	K7-90
P. R. Bredt	P7-25
J. W. Brothers (10)	K9-20
S. A. Bryan (10)	P7-25
L. L. Burger	P7-25
D. M. Camaioni	K2-44
J. A. Campbell	P8-08
C. D. Carlson	P7-25
S. V. Forbes	P7-25
P. A. Gauglitz	P7-41
S. C. Goheen	P8-08
R. T. Hallen	P8-38
C. M. King	P7-25
L. A. Mahoney	K7-15
L. R. Pederson	K2-44
W. D. Samuels	K2-44
R. D. Scheele	P7-25
R. L. Sell	P7-25
C. W. Stewart	K7-15
J. M. Tingey	P7-25
Information Release (5)	K1-06